

Fingerprint Image Segmentation Algorithm Based on Contourlet Transform Technology

Guanghua Zhang*, Zhongyang Xiong, Shuyin Xia,
Yueguo Luo, Changyuan Xing

College of Computer Science
Chongqing University
Area A, No. 174, Shazheng Str., Shapingba District
Chongqing, 400030, China
E-mails: guanghua0420@gmail.com, zyxiong@cqu.edu.cn,
yshxkkk@cqu.edu.cn, ygluo@cqu.edu.cn, cyxing@cqu.edu.cn

*Corresponding author

Received: February 16, 2016

Accepted: September 10, 2016

Published: September 30, 2016

Abstract: This paper briefly introduces two classic algorithms for fingerprint image processing, which include the soft threshold denoise algorithm of wavelet domain based on wavelet domain and the fingerprint image enhancement algorithm based on Gabor function. Contourlet transform has good texture sensitivity and can be used for the segmentation enforcement of the fingerprint image. The method proposed in this paper has attained the final fingerprint segmentation image through utilizing a modified denoising for a high-frequency coefficient after Contourlet decomposition, highlighting the fingerprint ridge line through modulus maxima detection and finally connecting the broken fingerprint line using a value filter in direction. It can attain richer direction information than the method based on wavelet transform and Gabor function and can make the positioning of detailed features more accurate. However, its ridge should be more coherent. Experiments have shown that this algorithm is obviously superior in fingerprint features detection.

Keywords: Fingerprint image segmentation algorithm, Contourlet transform.

Introduction

Image segmentation is the basis of image understanding, analysis and recognition. The effect of image segmentation directly affects the performance of subsequent image processing, thus making it a key issue in the field of image processing. However, making image segmentation on multi-scale with adoption of wavelet transform can attain corresponding segmentation of an image at each scale, but two-dimensional separable wavelet is formed by one-dimensional wavelet. Its primary function is isotropic and has only limited direction, which can only detect the point singularity, but cannot effectively detect the line singularity and surface singularity in a two-dimensional image [10].

Contourlet transform is a “real” image two-dimensional expression method, which has attained extensive attention from an increasing number of scholars and achieved very good effects in each facet in the field of image processing [11, 12]. Contourlet transform has multi-resolution time-frequency analysis features of wavelet transform, as well as a flexible multi-directional and anisotropic scaling relationship [20]. Compared with the wavelet transform method, Contourlet transform technology can set various direction numbers in the directional filter bank at each layer, and therefore can capture more directional information [1, 15].

Materials and methods

Contourlet transform is realized by Laplacian Pyramid and directional filter, which has multi-resolution time-frequency analysis features of wavelet transform, as well as high multi-directional and anisotropic scaling relationship [4]. Compared with the wavelet transform method, Contourlet can set the direction number in the directional filter bank at each layer, and therefore can capture more direction information [17]. Theoretically speaking, Contourlet transform is more suitable for fingerprint image processing and can achieve a better effect [6, 16]. This paper has established a new fingerprint image segmentation method through a high frequency sub-band adaptive correction factor after fingerprint image Contourlet change and detected module maximum, while at the same time, connecting the broken fingerprint ridge line by adopting block directional information [5]. Experiments have found that this method is superior in details extraction of a fingerprint image and has practical value [22]. The algorithm flow chart is as shown in Fig. 1.

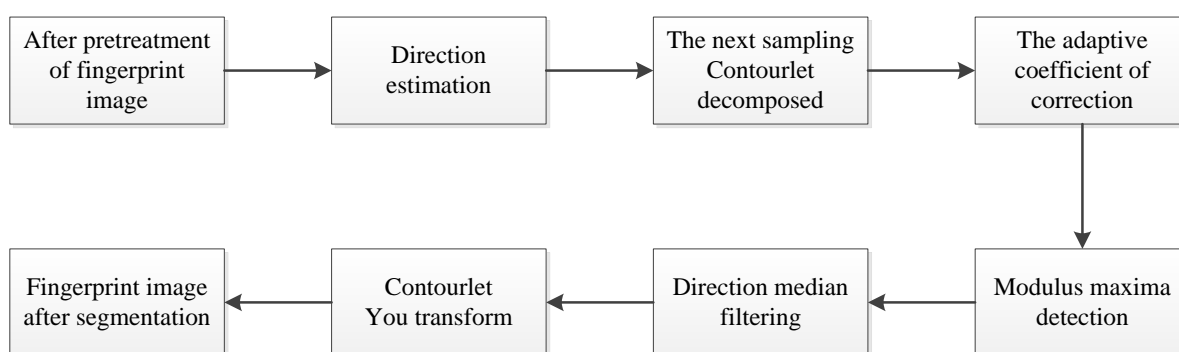


Fig. 1 Fingerprint image segmentation based on Contourlet transform process

Orientation estimation

Because a fingerprint ridge has fixed directional information, the calculation at fingerprint ridge direction is essential to fingerprint image processing [18]. To decrease the complexity of calculation, this paper calculates direction through a local fingerprint image. The fingerprint image is divided into blocks of the same size. The size of block is determined by the fingerprint direction within the block, thus ensuring that the fingerprint direction of each block is single [8]. Meanwhile, the fingerprint direction is quantized into eight blocks, as shown in Fig. 2.

Based on the above description, the gradient direction of the fingerprint ridge line is assumed to be the minimum, then the direction of each block can be calculated based on the following steps:

- (1) Divide the fingerprint image into the block whose size is $T \times T$, and select T as 8 or 16.
- (2) Calculate the gradient of each pixel point in eight directions within each block by using the Sobel algorithm; indicates eight directions [7].
- (3) Calculate the sum of the gradient of each pixel point in eight directions within each block. Regard the gradient and minimum direction as the fingerprint ridge direction of this block.

The above steps can determine that the direction of the fingerprint ridge can be calculated based on the following formula:

$$\theta = \arg \min_k \left\{ \sum_{(i,j) \in W} g(i,j,k) \right\} \tag{1}$$

in which, W is a sub-block image.

The direction of each block of the fingerprint image can be attained based on above steps.

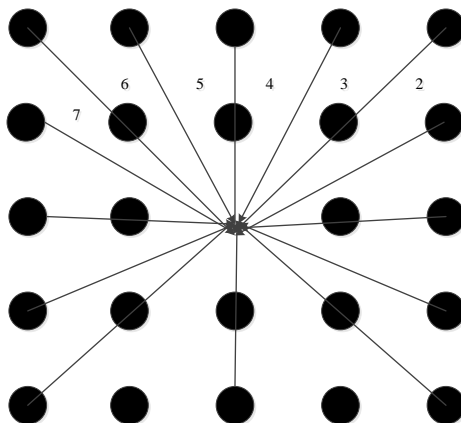


Fig. 2 Direction quantitative figure

Non-subsampled Contourlet transform (NSCT)

Because down sampling treatment in Contourlet transform will reduce the resolution of the image, for the 16×16 blocks in this paper, the continuous decreasing of resolution will cause difficulty to the subsequent treatment [3]. Therefore, this paper adopts NSCT. When using NSCT, all the pixel points in the sub-generation image are matched one-to-one, and the pixel points in the sub-generation image and the original image are the same at the time domain position. The process of NSCT is as shown in Fig. 3.

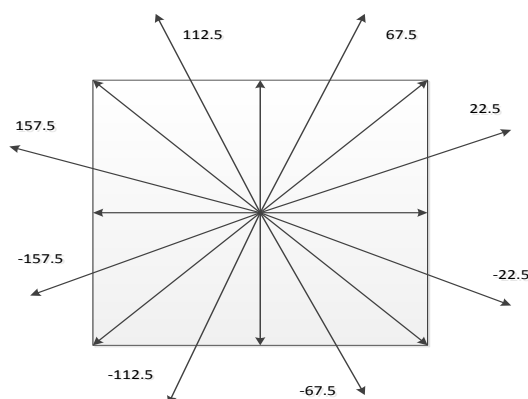


Fig. 3 Sub-band equivalent gradient directions

Contourlet coefficient and fingerprint image

In observing a fingerprint image, it is obvious that the fingerprint has direction, which means that fingerprint ridge has a geometric structure while noise does not. Based on above observation, we find that it is similar to the wavelet decomposition coefficient; the smooth region of the image corresponds to the non-significant coefficient with a small value, while the local features of the image, such as the ridge, corresponds to the significant coefficient with a larger amount of data [13]. Compared with wavelet coefficient, the more outstanding

characteristic of Contourlet coefficient is: for specific directions of sub-band, only the image in the certain direction will have significant coefficients

Because all the Contourlet coefficients in the sub-band correspond to the original image pixels position, the ridge information at each direction in the fingerprint image distributes in the high-frequency sub-band coefficient after transform. Therefore, the geometric feature of each pixel can be easily attained through the Contourlet sub-band coefficient [2].

High-frequency sub-band coefficients can be divided into three categories, which include the strong edge coefficient, the weak edge coefficient and the interference coefficient [9, 19, 21]. Under the same scale, the strong edge coefficient nearly presents a large mode value in all corresponding positions of the sub-bands; the weak edge coefficient only presents a large mode value in some sub-bands of specific directions and the mode value at the corresponding position at other directions are small, while for interference value, the corresponding mode value in sub-bands of all directions is small.

The coefficient modulus of each pixel at each direction can be calculated based on this, and its mean value and max values are calculated. The category of the sub-band coefficient can be distinguished through setting a suitable threshold value $c\sigma$, which includes the strong edge coefficient, the weak edge coefficient and the noise coefficient.

$$\begin{cases} \text{strong edge,} & \text{if } mean \geq c\sigma \\ \text{weak edge,} & \text{if } mean < c\sigma, \max \geq c\sigma \\ \text{noise,} & \text{if } mean < c\sigma, \max < c\sigma \end{cases} \quad (2)$$

in which, max is the max coefficient mode value within filtering window $(2M + 1) \times (2N + 1)$. In this paper, because the fingerprint ridge width is about five pixels, the values of M and N are set at 5, while the mean value can be calculated based on following formula:

$$mean = \frac{1}{(2M + 1)(2N + 1)} \sum_{m=i-M}^{i+M} \sum_{n=j-N}^{j+N} I(m, n) \quad (3)$$

$$\sigma = \frac{1}{(2M + 1)(2N + 1)} \sum_{m=i-M}^{i+M} \sum_{n=j-N}^{j+N} (I(m, n) - mean(m, n))^2 \quad (4)$$

Therefore, the Contourlet coefficient can be corrected through Eq. (4) based on the classification of each pixel, and thus strengthening the weak edge and restricting noise.

$$y(x) = \begin{cases} x, & \text{strong edge pixels} \\ \max \left(\left(\frac{c\sigma}{|x|} \right)^{0.5}, 1 \right) x, & \text{weak edge pixels} \\ 0, & \text{noise pixels} \end{cases} \quad (5)$$

in which, x is the original Contourlet coefficient. Through the above steps, the strong edge coefficient is retained and the weak edge coefficient is enlarged, and the interference coefficient is set at 0.

It needs to be noted that adaptive filtering window is made along the block fingerprint direction of the above calculation.

Modulus maxima detection

Modulus maxima detection extracts a high-efficiency coefficient through check modulus maxima, outline the fingerprint ridge and attain a complete high-frequency fingerprint image through the method modulus maxima detection [22].

The traditional modulus maxima detection method based on wavelet needs to calculate the phase angle of the modulus to confirm the direction of the curve gradient, while the filter bank of Contourlet transform cannot be separated. Its coefficient of sub-band at each direction already includes adequate directional information that is specific directional sub-band, including modulus maxima at a specific direction. Therefore, it can simplify the calculation of Contourlet transform modulus maxima.

It can be judged if one point $Coeffs_{i,k}^i(n)$ in the sub-band coefficient at one direction is modulus maxima point by i grade sub-band equivalent gradient decomposition, and the direction number of decomposition of each grade is eight, as an example (other situations are similar). In Fig. 4, parameter n divided by the j grade decomposition is the pixel coordinates of the sub-band at k direction. Fig. 4 shows that each $Coeffs_{i,k}^i(n)$ in directional sub-band, can be used to be the equivalent gradient direction of the edge along $ArgCoeffs_{i,k}^i(n)$ direction. Then, compare the modulus of two adjacent elements at equivalent gradient directions corresponding to $\text{mod}[Coeffs_{i,k}^i(n)]$ and $ArgCoeffs_{i,k}^i(n)$, and confirm if the modulus at this point is local maximum. That is:

$$\text{mod}[Coeffs_{i,k}^i(n_1, n_2)] = \begin{cases} 0, & \text{mod}[Coeffs_{i,k}^i(n_1, n_2)] < \text{mod}[Coeffs_{i,k}^i(n_1 - r_1(n_1), n_2 - r_1(n_2))] \\ 0, & \text{mod}[Coeffs_{i,k}^i(n_1, n_2)] < \text{mod}[Coeffs_{i,k}^i(n_1 - r_2(n_1), n_2 - r_2(n_2))] \\ \text{mod}[Coeffs_{i,k}^i(n_1, n_2)], & \text{otherwise} \end{cases} \quad (6)$$

First, the coefficient modulus maxima detection is made for sub-band at each direction of each scale, and then the suitable threshold treatment for modulus maxima matrix is made, and finally Contourlet inverse transform is made for the processed coefficient matrix; at this moment, fingerprint segmentation image can be attained after binarization treatments.

Directional median filter

A high-frequency fingerprint image presents more detailed features but the ridge has poor continuity. To connect the discontinuity phenomenon of the ridge after high-frequency treatment, a directional median filter has been adopted in this paper. When median filter treatment is made for one pixel point $I(i, j)$, it can be found that:

$$Y(i, j, W) = \text{median}(I_{i-k}, \dots, I_{i,j}, \dots, I_{i+k, j+1}) \quad (7)$$

where W is the median filter window whose size can be adjusted.

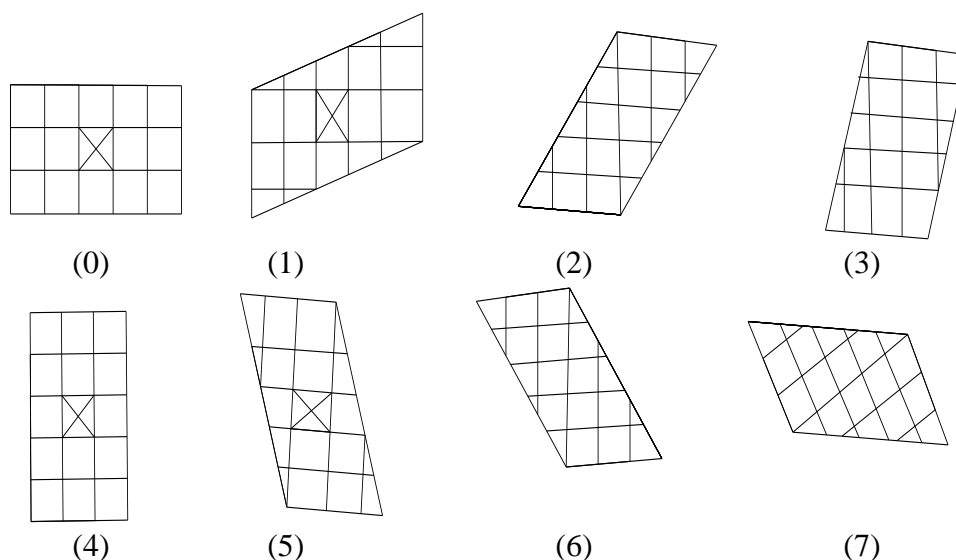


Fig. 4 Eight direction median filtering window templates

In fingerprint image processing, it is difficult for a standard median filter to produce an obvious effect, because the fingerprint image has unique line features, with direction slowly and smoothly changing. However, the pixels between broken ridge lines can be regarded as impulse noise, so the median filter with the same filtering direction and ridge direction can reduce the interference effectively; that is, to connect the broken fingerprint ridge line. To make the median filter direction cooperate with the ridge direction of the fingerprint, the shape of filter window can be changed. Based on the eight directions set shown in Fig. 4, the shape of the corresponding median filter window is as shown in Fig. 4(5).

The median filter window is set at 3×7 based on the fact that the width of broken fingerprint line is about 3 pixel points and the length is about 5-7 pixel points.

Results and discussion

This experiment conducts a simulation under Matlab 7.6 environment and adopts a gray level fingerprint image as the experimental image. The algorithm in this paper makes two grades Contourlet transform for the fingerprint image, the number of sub-bands at high-frequency level is eight, LP decomposition and DFB decomposition adopt 9-7 filter and PKVA filter respectively.

To verify the effectiveness of this algorithm, it is compared with the soft-threshold value algorithm based on wavelet as well as the fingerprint enforcement algorithm based on Gabor filter [14]. Wavelet transform adopts db4 wavelet base and makes two-layer decomposition. The blocking size of Gabor filter is 16×16 . The comparison results are as shown in Figs. 7, 8 and 9.

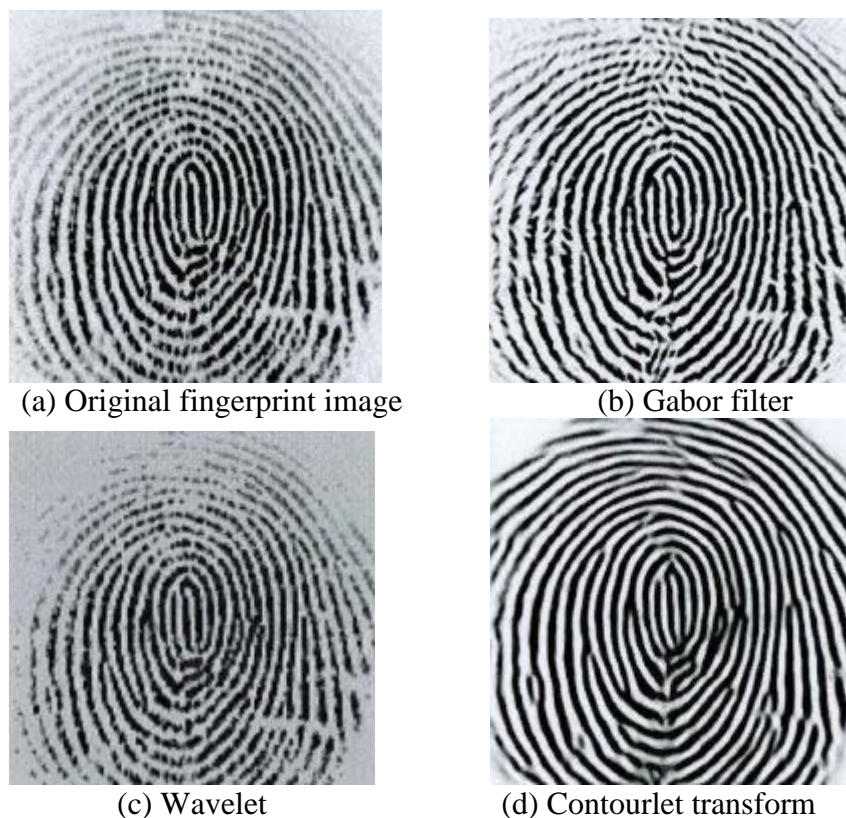


Fig. 5 Comparison 1 of different fingerprint processing algorithm

The above demonstrates that the wavelet algorithm can detect the fingerprint information more accurately. It partially removes interference and improves the quality of fingerprint image. However, the fingerprint ridge line after processing is does not have good continuity, and it also partially loses some useful information in the fingerprint image denoising process. Therefore, the overall improvement effect is not obvious. Gabor filtering will produce additional noise at particular direction, which makes the fingerprint image only able to be effectively strengthened at some parts while producing extra noise at other parts. The algorithm in this paper can effectively reduce noise, and the fingerprint ridge line has good continuity.

To further verify the effectiveness of this algorithm, binarization and refinement are utilized to make feature detection for this algorithm, and wavelet soft closed value shareholding algorithm is used as well as the fingerprint image after filtering treatment. Fig. 5 are fingerprint images after linearization. Figs. 6, 7 and 8 are images for refinement and feature detection.

Careful observation of the above detected features reveals that compared with the other two methods, fingerprint image segmentation algorithm based on Contourlet decomposition proposed in this paper has more accurate positioning for detailed features of the fingerprint image, the detected pseudo features are less and the overall effect is good.

The spectral fingerprint image at the optimal spectrum is processed using the fingerprint image segmentation algorithm based on Contourlet and the segmentation image is shown in Fig. 9. Its binary image after simple treatment and binarization is shown in Fig. 10.

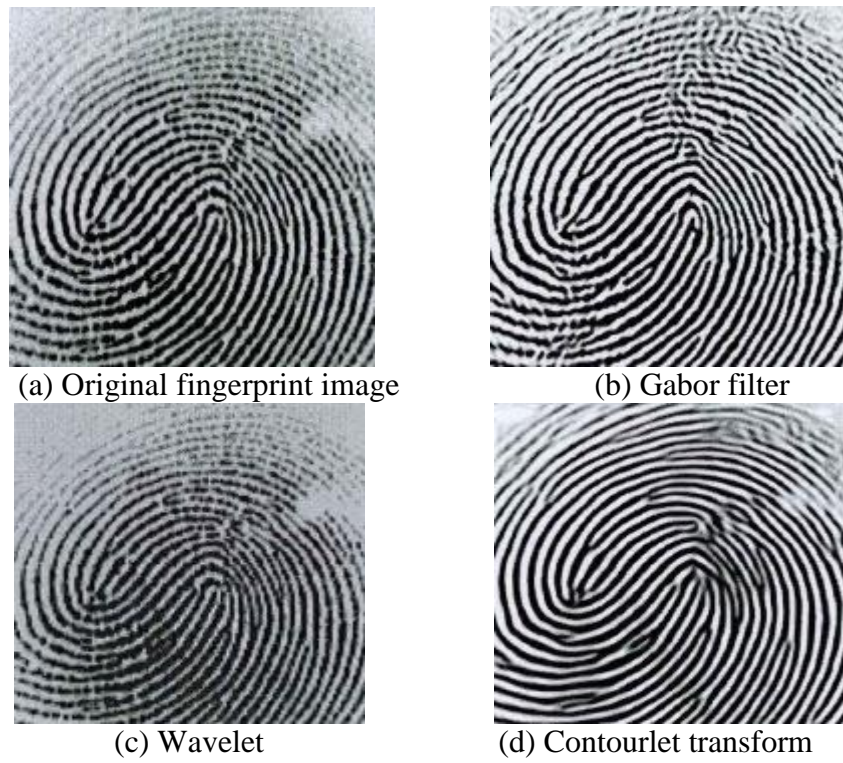


Fig. 6 Comparison 2 of different fingerprint processing algorithm

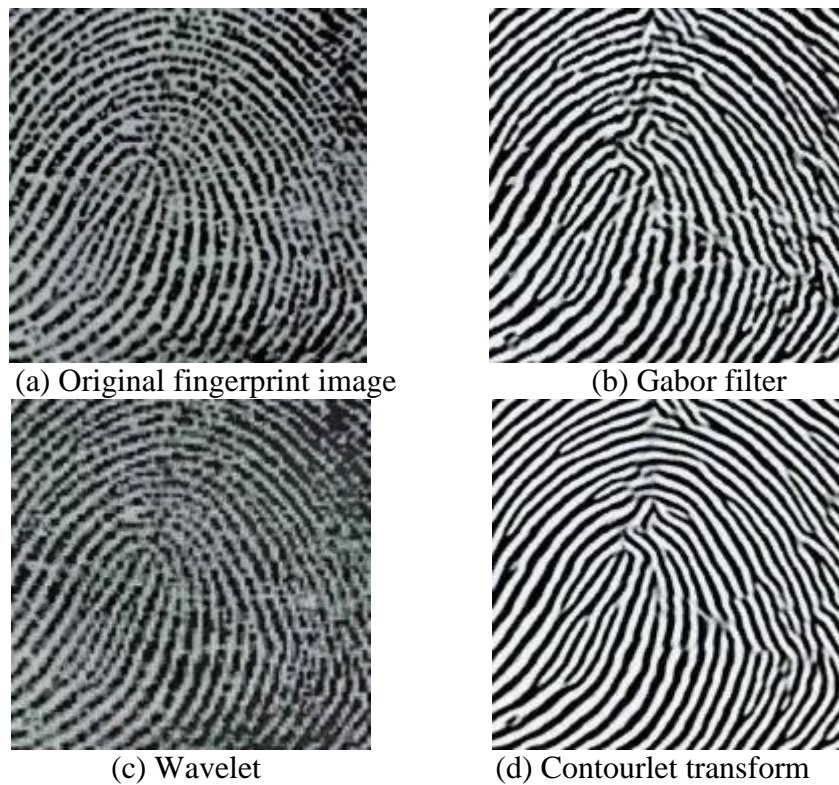


Fig. 7 Comparison 3 of different fingerprint processing algorithm

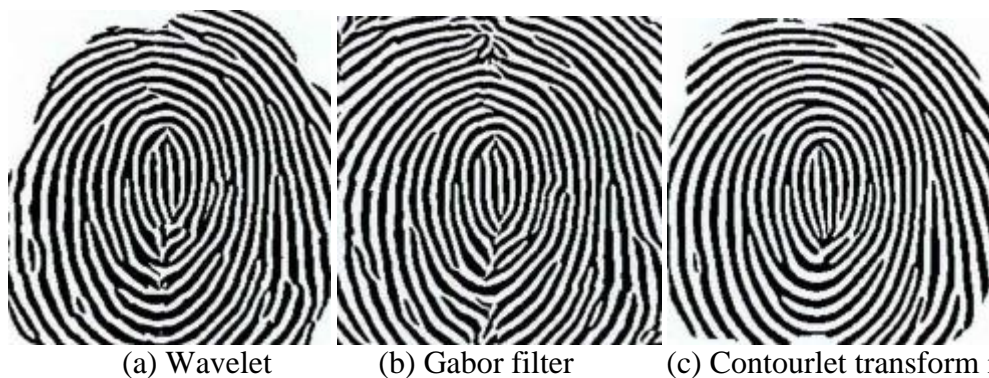


Fig. 8 Differences algorithm comparison 1 of fingerprint binarization processing

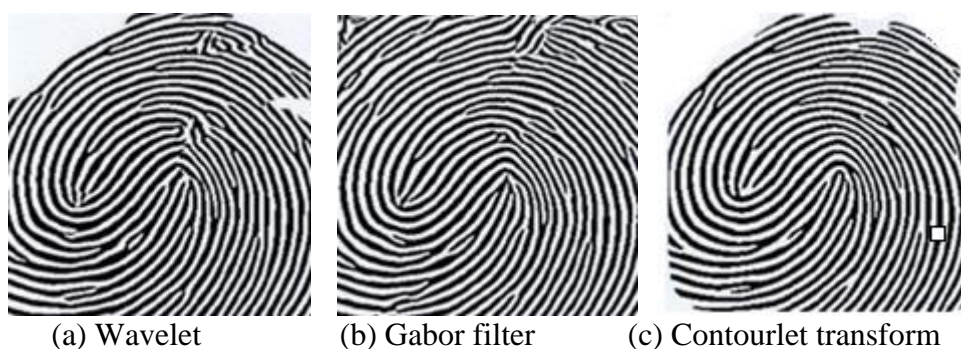


Fig. 9 Differences algorithm comparison of fingerprint binarization processing

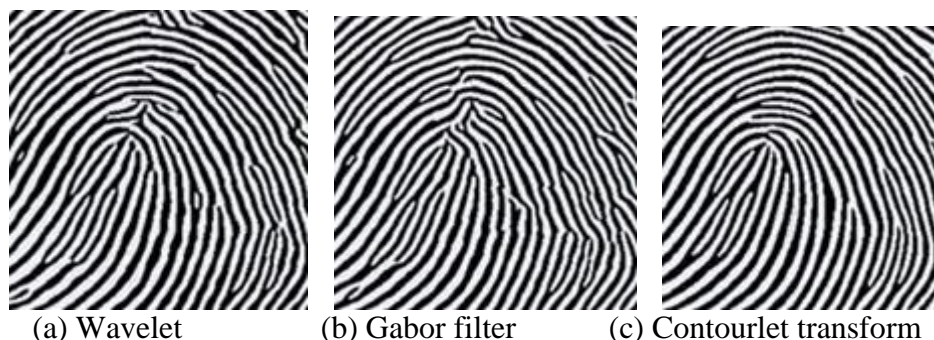


Fig. 10 Differences algorithm comparison 3 of in fingerprint binarization processing

Conclusion

This paper has made a brief introduction of two classic algorithms for fingerprint image processing, which include the soft closed value denoising algorithm based on wavelet domain and the fingerprint image enhancement algorithm based on Gabor function, and it has pointed out their features through theoretical analysis and deduction.

Contourlet transform has good texture sensitivity and can be used for the segmentation enforcement for fingerprint images. The method proposed in this paper has attained the final fingerprint segmentation image through utilizing a modified denoising for high-frequency coefficient after Contourlet transform, highlighting the fingerprint ridge line through modulus maxima detection and finally connecting the broken fingerprint line using a value filter in direction. It can attain richer direction information than the method based on wavelet transform and Gabor function and make the positioning of detailed features more accurate.

However, its ridge should be more coherent. Experiments have shown that this algorithm is obviously superior in fingerprint feature detection.

References

1. Abhyankar A., S. Schuckers (1998). Integrating a Wavelet Based Perspiration Liveness Check with Fingerprint Recognition, *Pattern Recognition*, 42(3), 452-464.
2. Bazen A. M., S. H. Gerez (2001). Segmentation of Fingerprint Images, *Prorisc Workshop on Circuits Systems & Signal Processing*, 276-280.
3. Blanton M., P. Gasti (2011). Secure and Efficient Protocols for Iris and Fingerprint Identification, *Computer Security – ESORICS 2011, 16th European Symposium on Research in Computer Security*, Leuven, Belgium, September 12-14, 190-209.
4. Cappelli R., M. Ferrara, D. Maltoni (2010). Minutia Cylinder-code: A New Representation and Matching Technique for Fingerprint Recognition, *IEEE Transactions on Pattern Analysis & Machine Intelligence*, 32(12), 2128-2141.
5. Cole S. A. (2005). Accounting for Error in Latent Fingerprint Identification, *Journal of Criminal Law & Criminology*, 95(3), 985-1078.
6. Egli Anthonioz N. M., C. Champod (2014). Evidence Evaluation in Fingerprint Comparison and Automated Fingerprint Identification Systems – Modeling between Finger Variability, *Forensic Science International*, 235(2), 86-101.
7. Egli N. M., C. Champod, P. Margot (2007). Evidence Evaluation in Fingerprint Comparison and Automated Fingerprint Identification Systems – Modelling within Finger Variability, *Forensic Science International*, 167(2-3), 189-95.
8. Fielding K. H., J. L. Horner, C. K. Makekai (1990). Optical Fingerprint Identification by Binary Joint Transform Correlation, *Optical Engineering*, 30(12), 1958-1961.
9. Hong L., Y. Wan, A. Jain (1998). Fingerprint Image Enhancement: Algorithm and Performance Evaluation, *IEEE Transactions on Pattern Analysis & Machine Intelligence*, 20(8), 777-789.
10. Hrechak A. K., J. A. Mchugh (1990). Automated Fingerprint Recognition Using Structural Matching, *Pattern Recognition*, 23(8), 893-904.
11. Isenor D. K., S. G. Zaky (1986). Fingerprint Identification Using Graph Matching, *Pattern Recognition*, 19(2), 113-122.
12. Jea T. Y., V. Govindaraju (2005). A Minutia-based Partial Fingerprint Recognition System, *Pattern Recognition*, 38(10), 1672-1684.
13. Li X., H. Lu, M. Wang (2013). A hybrid Gene Selection Method for Multi-category Tumor Classification Using Microarray Data, *International Journal Bioautomation*, 17(4), 249-258.
14. Marasco E., A. Ross (2014). A Survey on Antispoofing Schemes for Fingerprint Recognition Systems, *ACM Computing Surveys*, 47(2), 1-36.
15. Putte T. V. D., J. Keuning (2000). Biometrical Fingerprint Recognition: Don't Get Your Fingers Burned, *Proceedings of the Fourth Working Conference on Smart Card Research and Advanced Applications, CARDIS 2000*, 52, 289-303.
16. Tico M., P. Kuosmanen, J. Saarinen (2001). Wavelet Domain Features for Fingerprint Recognition, *Electronics Letters*, 37(1), 21-22.
17. Wahab A., S. H. Chin, E. C. Tan (1998). Novel Approach to Automated Fingerprint Recognition, *IEE Proceedings – Vision Image and Signal Processing*, 145(3), 160-166.
18. Wang Y., J. Hu (2011). Global Ridge Orientation Modeling for Partial Fingerprint Identification, *IEEE Transactions on Pattern Analysis & Machine Intelligence*, 33(1), 72-87.
19. Wein L. M., B. H. Singer (2005). Using Fingerprint Image Quality to Improve the Identification Performance of the U.S. Visitor and Immigrant Status Indicator Technology

- Program, Proceedings of the National Academy of Sciences of the United States of America, 102(21), 7772-7775.
20. Willis A., L. Myers (2001). Cost-effective Fingerprint Recognition System for Use with Low-quality Prints and Damaged Fingertips, *Pattern Recognition*, 34(2), 255-270.
 21. Xiao Q., H. Raafat (1991). Fingerprint Image Postprocessing: A Combined Statistical and Structural Approach, *Pattern Recognition*, 24(10), 985-992.
 22. Yeung M. M., S. Pankanti (2000). Verification Watermarks on Fingerprint Recognition and Retrieval, *Proceedings of SPIE – The International Society for Optical Engineering*, 9(4), 468-476.

Guanghua Zhang, Ph.D. Student

E-mail: guanghua0420@gmail.com



Guanghua Zhang received his B.Sc. degree in computer science from Changchun University of Science and Technology in 2008, and M.Sc. degree from University of Science and Technology of China in 2011. He is currently studying for his Ph.D. degree in College of Computer Science in Chongqing University in China. His research interests include pattern recognition, image processing, and computer vision.

Prof. Zhongyang Xiong, Ph.D.

E-mail: zyxiong@cqu.edu.cn



Zhongyang Xiong is a Professor at College of Computer Science in Chongqing University and the Dean of Information and Campus Network Management Center. He received the B.Sc. degree of engineering in 1985, the M.Sc. degree in 1988, and his Ph.D. in Engineering in 2004, all in College of Computer Science in Chongqing University in China. His research interests include data mining, pattern recognition, computer network and cloud computing.

Shuyin Xia, Ph.D.

E-mail: xiasy@cqupt.edu.cn



Shuyin Xia received his B.Sc. degree in Engineering in 2008, and M.Sc. degree in 2012, both in Computer Science from Chongqing University of Technology in China. He received his Ph.D. degree in College of Computer Science in Chongqing University in China. He is currently a lecturer at College of Computer Science and Technology, Chongqing University of Posts and Telecommunications. His research interests include data mining, computational intelligence and machine learning.

Yueguo Luo, Ph.D. Student

E-mail: ygluo@cqu.edu.cn



Yueguo Luo received his B.Sc. degree from Beihua University in China in 2004, and the M.E. degree from Chongqing University in China in 2009, both in Computer Science. He is currently working toward his Ph.D. degree in Chongqing University, as well as teaching in Yangtze Normal University in China. His research interests include data mining and computational intelligence.

Changyuan Xing, Ph.D.

E-mail: cyxing@cqu.edu.cn



Changyuan Xing received his B.Sc. degree in 2005, M.Sc. degree in 2009, and his Ph.D. degree of computer science from Chongqing University in 2015. His research interests include pattern recognition, image processing and computer vision.